

## APPLIED SCIENCES AND ENGINEERING

# Performing calculus: Asymmetric adaptive stimuli-responsive material for derivative control

Spandhana Gonuguntla<sup>1\*</sup>, Wei Chun Lim<sup>1\*</sup>, Fong Yew Leong<sup>2</sup>, Chi Kit Ao<sup>1</sup>, Changhui Liu<sup>1</sup>, Siowling Soh<sup>1†</sup>

Materials (e.g., brick or wood) are generally perceived as unintelligent. Even the highly researched “smart” materials are only capable of extremely primitive analytical functions (e.g., simple logical operations). Here, a material is shown to have the ability to perform (i.e., without a computer), an advanced mathematical operation in calculus: the temporal derivative. It consists of a stimuli-responsive material coated asymmetrically with an adaptive impermeable layer. Its ability to analyze the derivative is shown by experiments, numerical modeling, and theory (i.e., scaling between derivative and response). This class of freestanding stimuli-responsive materials is demonstrated to serve effectively as a derivative controller for controlled delivery and self-regulation. Its fast response realizes the same designed functionality and efficiency as complex industrial derivative controllers widely used in manufacturing. These results illustrate the possibility to associate specifically designed materials directly with higher concepts of mathematics for the development of “intelligent” material-based systems.

## INTRODUCTION

Despite the advances of materials through many years of research, the analytical functions that can be performed by materials are still very primitive, especially when compared to biological and electronic systems (1, 2). Advanced analytical and mathematical functions are necessary for a wide range of applications. One important application is a controller for regulating processes. Control of processes is important in a vast range of circumstances, including industry for manufacturing processes, laboratories for experiments, biological systems (e.g., regulating chemicals in and out of a cell), many types of daily activities (e.g., cooking), and the environment (e.g., conditions of soil). A large number of process variables (e.g., concentration, temperature, and pressure) usually need to be controlled. However, achieving good control is challenging because most practical processes are highly dynamic and unpredictable (3): Many common processes (e.g., the human body) involve a supply of substances that is highly variable and/or unknown (e.g., sudden intake of a large dose of sugar), uncontrollable external disturbances, and complex mechanisms that are not well understood. Hence, controllers need to be carefully designed for responding effectively to these challenging and unpredictable circumstances.

For large-scale production in industry, engineers have developed efficient and sophisticated controllers (3). Good controllers usually require advanced analysis and calculation of the process data—calculus is often needed. One of the most important types of calculus performed by controllers is the temporal derivative (3). The derivative controller calculates and responds to the rate of change of a process variable with time (i.e., the temporal gradient). A steeper temporal gradient causes the derivative controller to produce a larger response, and vice versa (Fig. 1A; responses “1” and “2”). Its importance can be illustrated by a typical situation in which

a process variable is rapidly increasing at the current time (i.e., a large temporal gradient) but needs to be controlled within a threshold limit (e.g., a threshold temperature before a runaway reaction occurs; Fig. 1, B and C). If the control involves simply detecting and responding proportionally to the process variable at the current time point (Fig. 1B), the response from the controller may be too late: The variable may quickly exceed the limit, thus leading to potentially undesirable consequences. On the other hand, a sharp temporal gradient, even when the process variable is still well within the limits, indicates that the variable will likely exceed the limit in the near future. Through detecting the sharp temporal gradient, the derivative controller produces a large response and brings the process variable back to its desired level (i.e., the set point) rapidly (Fig. 1C). A specific example is the regulation (e.g., releasing of drugs) of the condition of a system (e.g., the human body) by responding to the changes in the concentration of a chemical in a liquid medium (e.g., the level of glucose). If a very sharp spike in the concentration occurred (i.e., a large temporal derivative) even when the concentration is still within reasonable limits, it would be desirable for the system to regulate with a correspondingly large response to counteract the increase (e.g., to quickly bring down the glucose levels before unhealthy limits are exceeded). The derivative controller thus has the ability to pre-emptively rectify a potentially undesirable situation—it “predicts the future” (3). Because of this unique feature, the derivative control is one of the most important and common strategies used in controllers across all types (e.g., petrochemical, chemical, and pharmaceutical) of industries. One main feature of the derivative control is that it provides a zero response whenever the variable is constant with time (i.e., no gradient). The response is zero regardless of the absolute magnitude of the variable (Fig. 1A; responses “3” and “4”).

However, controllers are complex: They generally require many components (e.g., sensors, actuators, converters, and wiring), tethered sources of energy (e.g., electricity or air pressure for pneumatic actuation), skilled personnel for operation, difficult installation, and expensive and bulky equipment. The high level of sophistication and cost of these controllers have greatly limited their

Copyright © 2021  
The Authors, some  
rights reserved;  
exclusive licensee  
American Association  
for the Advancement  
of Science. No claim to  
original U.S. Government  
Works. Distributed  
under a Creative  
Commons Attribution  
NonCommercial  
License 4.0 (CC BY-NC).

<sup>1</sup>Department of Chemical and Biomolecular Engineering, National University of Singapore, 4 Engineering Drive 4, Singapore 117585, Singapore. <sup>2</sup>A\*STAR Institute of High Performance Computing, 1 Fusionopolis Way, Connexis, Singapore 138632, Singapore.

\*These authors contributed equally to this work.

†Corresponding author. Email: chessl@nus.edu.sg

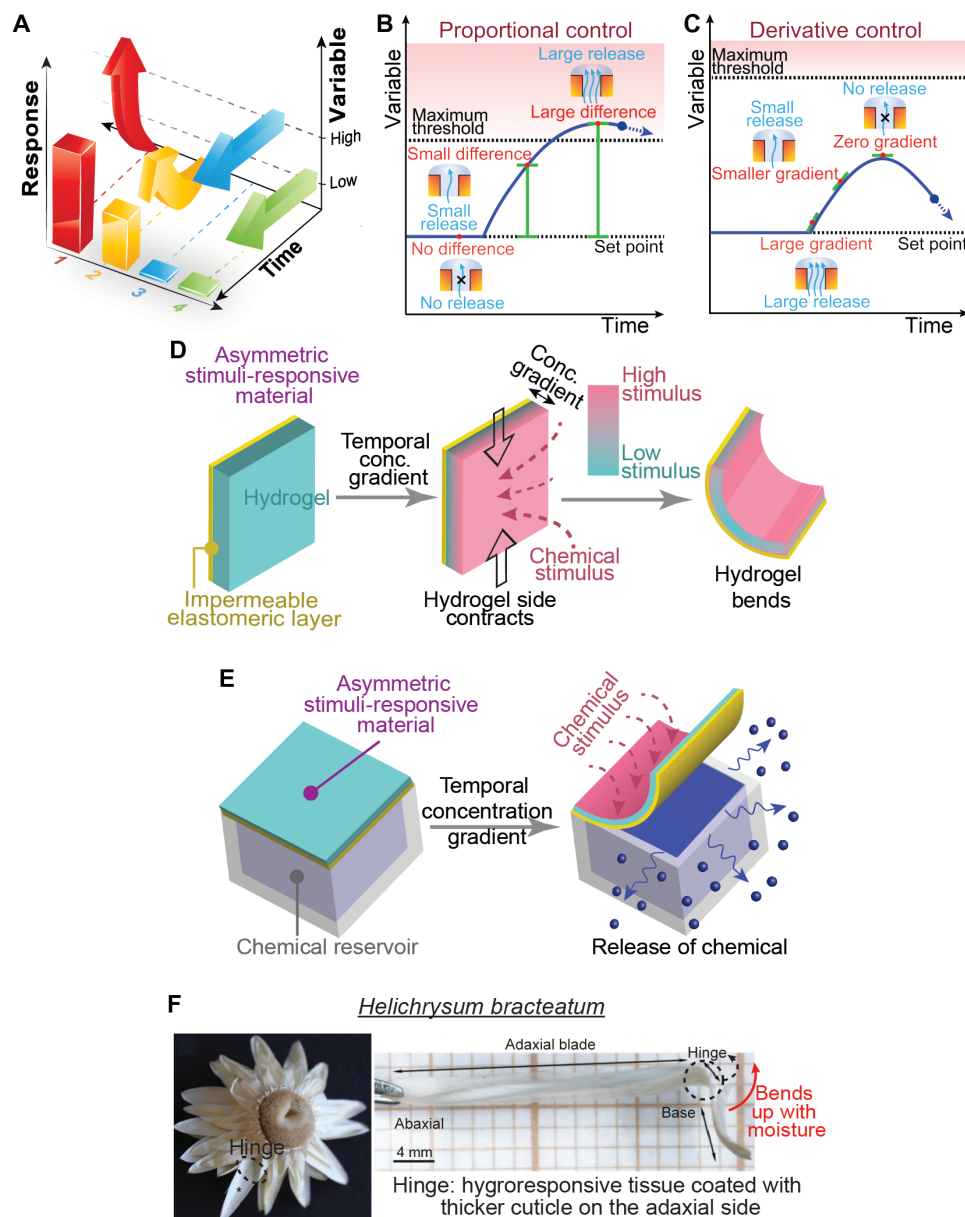


**Fig. 1. Asymmetric stimuli-responsive material that senses the temporal derivative of a process variable for derivative control.** (A) The definition of derivative control. (B) The proportional controller. The variable may easily exceed the maximum threshold if the response from the controller is directly proportional to the changes in the process variable due to the disturbance. (C) The derivative controller: It predicts the future trend and is capable of providing a fast corrective response before the process variable reaches unhealthy levels. (D) Stimuli-responsive hydrogel coated with a layer of impermeable elastomer (i.e., the asymmetric stimuli-responsive material) senses the temporal derivative of a chemical in the medium and responds by bending. (E) The bending actuation of the asymmetric stimuli-responsive material based on the temporal derivative can be used as a derivative controller for controlled delivery of a drug or chemical from a reservoir and self-regulation. (F) *H. bracteatum* is an example from nature that has a similar structure (image on the left). It consists of hygroresponsive hinges with thicker cuticles on one side that allows it to bend (image on the right). This image is reproduced with permission from Oxford University Press (31).

applications to mainly large-scale manufacturing processes. A computer is currently always needed for determining the temporal derivative of the process variable. It is thus usually not practical to use controllers for regulating the diverse range of common processes; examples include batch processes, nonstandardized ad hoc processes, relatively simple small-scale operations, and/or regions that are large (e.g., controlling the pH of vast areas of farmland). In addition, bulky electronic equipment cannot be used in many circumstances,

including environments that are highly inaccessible, harsh (e.g., corrosive), and incompatible with the electronic components (e.g., not biocompatible for use in the human body).

Hence, it would be ideal if controllers can be fabricated simply based on a freestanding piece of material with all the necessary features of a controller, including detection, analysis, and response incorporated—this material can potentially be used in a much broader range of applications. First, materials (e.g., polymers) can

be fabricated to detect many different types of stimuli from their surrounding medium, including temperature, pressure, fields, gases, ions, and concentration of many types of chemicals (e.g., glucose and alcohol) and biomolecules (e.g., enzymes and antigens) (2, 4–6). These stimuli-responsive materials, also referred to as “smart” materials, have been used in many applications such as the controlled release of chemicals. However, the functionalities of stimuli-responsive materials are extremely primitive compared to industrial controllers: They respond by providing a burst release (7–10), a preprogrammed release without active interaction with the surrounding (11), a release only when the stimulus exceeds a simple threshold, or a release that is proportional to the amount of stimulus detected (12, 13). The most analytically advanced types of stimuli-responsive materials currently developed are possibly those that perform simple logical operations (14–18). However, it is still challenging to perform even the most elementary mathematical operations (e.g., full addition and subtraction) (1). In addition, the stimuli-responsive systems used for regulation reported previously include numerous disadvantages such as nonreversible response, leakage, and sophisticated fabrication of complex systems. The need for highly specific types of stimuli (e.g., chemicals not usually found in typical environments) and conditions (19–22) highly limited the applicability of these systems. Notably, more advanced concepts of mathematics—including the temporal derivative—have never been performed without the use of a computer before, regardless of methods.

This study showed that a material has the ability to determine the temporal derivative of a stimulus in a way that is analogous to evaluating the mathematical first derivative in calculus. Despite performing this advanced mathematical operation, the material that we fabricated is simple: It consists of only a slab of stimuli-responsive hydrogel coated asymmetrically on one surface with a layer of impermeable and adaptive elastomer (the “asymmetric stimuli-responsive material”; Fig. 1D). Operationally, this asymmetric stimuli-responsive material is first immersed in the medium for the analysis of the temporal derivative of the concentration of a specific chemical (i.e., the stimulus) in the medium. When the concentration of the chemical in the medium increases, diffusion of the chemical into the stimuli-responsive hydrogel causes it to contract. Because of the impermeable elastomer, however, the chemical diffuses into only one surface of the hydrogel. This one-sided diffusion causes the hydrogel to contract asymmetrically; hence, the asymmetric stimuli-responsive material bends. A faster rate of increase in concentration (i.e., a larger temporal derivative) gives rise to a larger diffusive flux of the chemical into the hydrogel and a faster rate of bending of the asymmetric stimuli-responsive material. When the concentration stops changing (i.e., zero temporal derivative), diffusion causes the concentration of the chemical to homogenize throughout the hydrogel. It thus contracts uniformly throughout and straightens out. The asymmetric stimuli-responsive material is flat regardless of the magnitude of the concentration as long as the temporal derivative is zero. We show that the bending actuation of the asymmetric stimuli-responsive material can be used as a sensor and controller for controlled delivery of drugs and self-regulation based on the temporal derivative of the stimulus (Fig. 1E).

Previous studies have reported the bending of stimuli-responsive bilayers (i.e., materials that consist of a stimuli-responsive layer and a nonresponsive layer) and stimuli-responsive materials with structural

gradients (e.g., cross-linking and porosity) (23–25). Many aspects of the bending have been investigated, such as different methods of applying the stimulus (e.g., directional or time-dependent application of the stimulus) and time taken to bend (26, 27). However, the amount of bending of these previously reported stimuli-responsive materials is always proportional to the magnitude (i.e., not the temporal derivative) of the stimulus (28–30), a feature

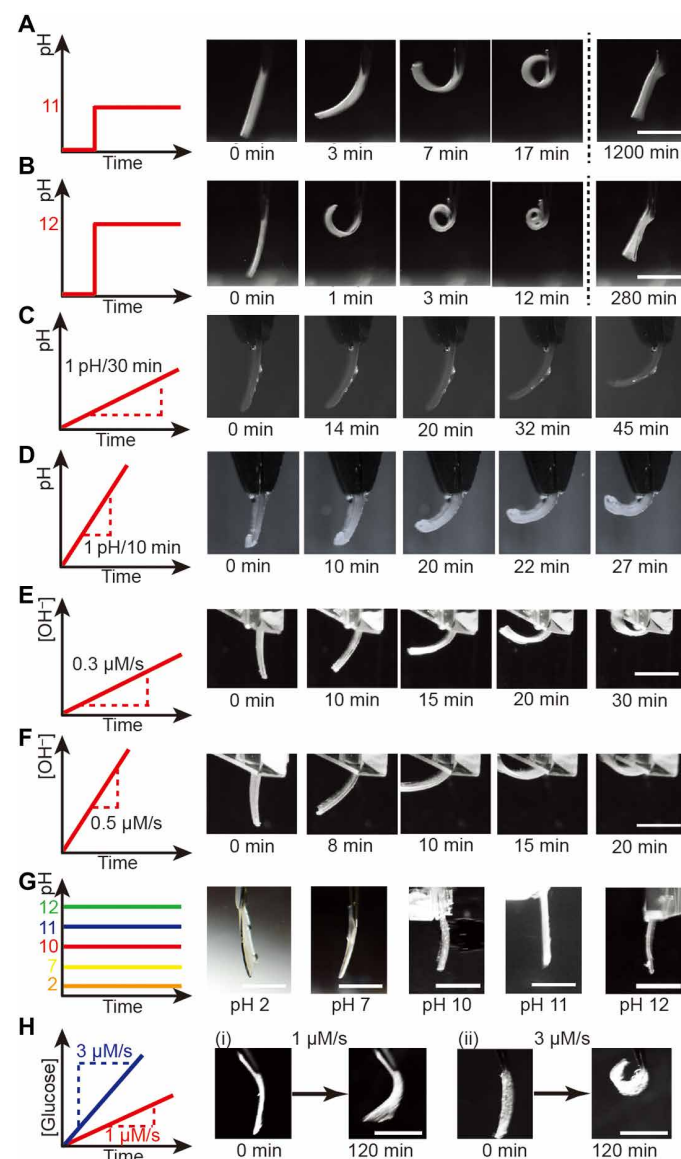


**Fig. 2. A derivative sensor.** The asymmetric pH-responsive material bent when the medium changed (A) rapidly from deionized water to pH 11, (B) rapidly from deionized water to pH 12, (C) with gradual linear increase of 1 pH unit per 30 min, (D) with gradual linear increase of 1 pH unit per 10 min, (E) gradually from deionized water to pH 11 by adding a pH 12 solution at 0.15 ml/min (or 0.3  $\mu\text{M/s}$ ), and (F) gradually from deionized water to pH 11 by adding a pH 12 solution at 0.25 ml/min (or 0.5  $\mu\text{M/s}$ ). (G) When the pH remained constant with time, the asymmetric pH-responsive material remained flat at pH 2, pH 7, pH 10, pH 11, or pH 12. (H) The asymmetric glucose-responsive material bent when a solution containing glucose (500 mg/dl) was added at a rate of (i) 0.1 ml/min (or 1  $\mu\text{M/s}$ ) or (ii) 0.3 ml/min (or 3  $\mu\text{M/s}$ ). Scale bars, 5 mm.



that is expected of stimuli-responsive materials for performing analytically simple functions. A characteristic of these materials is that they remain in the bent state as long as the stimulus of a specific magnitude is continuously being applied (i.e., including when there is no change in the stimulus). In our case, the asymmetric stimuli-responsive material that we prepared has a unique material property: The coating of elastomer is highly adaptive. Because of the highly adaptive nature of the layer of elastomer, it does not have any mechanical influence over the bending of the stimuli-responsive hydrogel; hence, the overall material can be regarded less as a “bilayer” but more as a stimuli-responsive material coated asymmetrically to be impermeable on one surface. This unique material property gives rise to the important feature of the asymmetric stimuli-responsive material that it remains in the flat state regardless of the magnitude of the stimulus as long as there is no change in stimulus. This important feature leads to the unexpected capability of the material to analyze the temporal derivative (and consequently, its ability to serve as a derivative controller and self-regulation) despite its simplicity. Its structure is inspired from intelligent systems commonly found in nature. One example involves the *Helichrysum bracteatum* that bends depending on the humidity (31). The hinges of the flower are made of hygroresponsive tissue coated with considerably thicker cuticle (i.e., an impermeable waxy layer) on one side (Fig. 1F). In this way, the moisture penetrates predominantly through the side opposite to the thick cuticle asymmetrically, thus allowing the hinge to bend.

## RESULTS

### Fabrication and performance of the asymmetric stimuli-responsive material

We fabricated the pH-responsive material by first polymerizing the pH-responsive hydrogel (i.e., based on the monomer *N*-*N*-dimethylaminoethylmethacrylate). Thereafter, we spin-coated a thin layer of the liquid elastomeric monomer onto one surface of the hydrogel and then polymerized the elastomer (figs. S1 and S2). The elastomer was found to be bonded with the hydrogel after polymerization. The chemical composition of the thin slab of asymmetric pH-responsive material (5 mm by 3 mm and a thickness of 160  $\mu\text{m}$  when fully expanded in pH 2 solution) was analyzed (see section S1, fig. S3, and table S1 for more details on the analysis).

Before the experiment, this asymmetric pH-responsive material was first fully expanded in an acidic medium. The acidic medium allowed the tertiary amine groups of the polymeric side chains of the pH-responsive hydrogel to become protonated; the repulsive forces between the charged groups of similar polarity of the polymeric chains caused the hydrogel to expand and absorb the aqueous solution from its surrounding medium. The asymmetric pH-responsive material was then immersed in deionized water as the initial condition before use. At equilibrium, it was flat in deionized water (Fig. 2A; image at  $t = 0$  min). Subsequently, we increased the concentration of  $\text{OH}^-$  ions by changing the medium to pH 11 rapidly at time  $t > 0$  (i.e., by removing the material from the deionized water and immediately immersing it in a pH 11 solution). In the basic medium, the

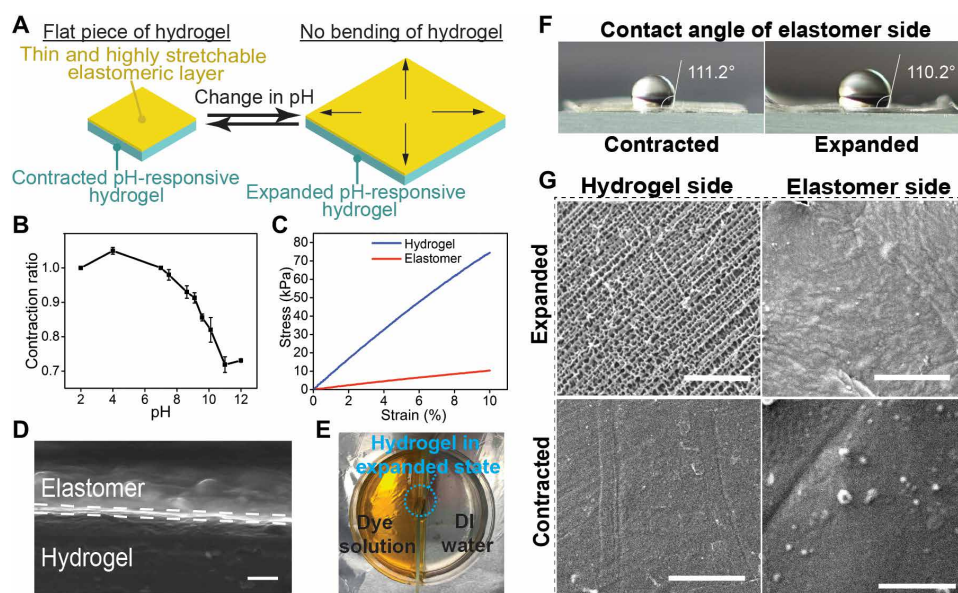


**Fig. 3. The smart and adaptive asymmetric pH-responsive material.** (A) The asymmetric pH-responsive material is smart: It responds to the change in pH by changing its size. The asymmetric pH-responsive material is adaptive due to its ability to remain flat regardless of its size (i.e., expanded or contracted). (B) Plot showing the contraction ratio of the asymmetric pH-responsive material at different pH at equilibrium. (C) Stress-strain curves of a slab of pH-responsive hydrogel and elastomer. (D) SEM image showed that the thickness of the coating of elastomer on the pH-responsive hydrogel was  $< 1 \mu\text{m}$ . Scale bar,  $10 \mu\text{m}$ . (E) The asymmetric pH-responsive material was impermeable to diffusion of molecules due to the coating of elastomer. It was used as a barrier for separating two reservoirs, one of which contained a yellow dye solution and the other contained deionized (DI) water. Even in its expanded state at pH 2, it prevented the diffusion of the dye from the reservoir on the left to the reservoir on the right. (F) Measurements of the contact angle of water on the surface of the pH-responsive hydrogel coated with the elastomer showed that the surface was always hydrophobic with approximately the same contact angle regardless of the size of the underlying hydrogel (i.e., both the expanded and contracted states). (G) SEM images of the surfaces of the slab of asymmetric pH-responsive material. Both the surface of the pH-responsive hydrogel (“hydrogel side”) and the surface coated with elastomer on the opposite side (“elastomer side”) are shown for the cases when the asymmetric pH-responsive material was expanded in a pH 2 solution and contracted in a pH 12 solution. Scale bars,  $200 \mu\text{m}$ . Photo credit: Spandhana Gonuguntla and Wei Chun Lim, National University of Singapore.

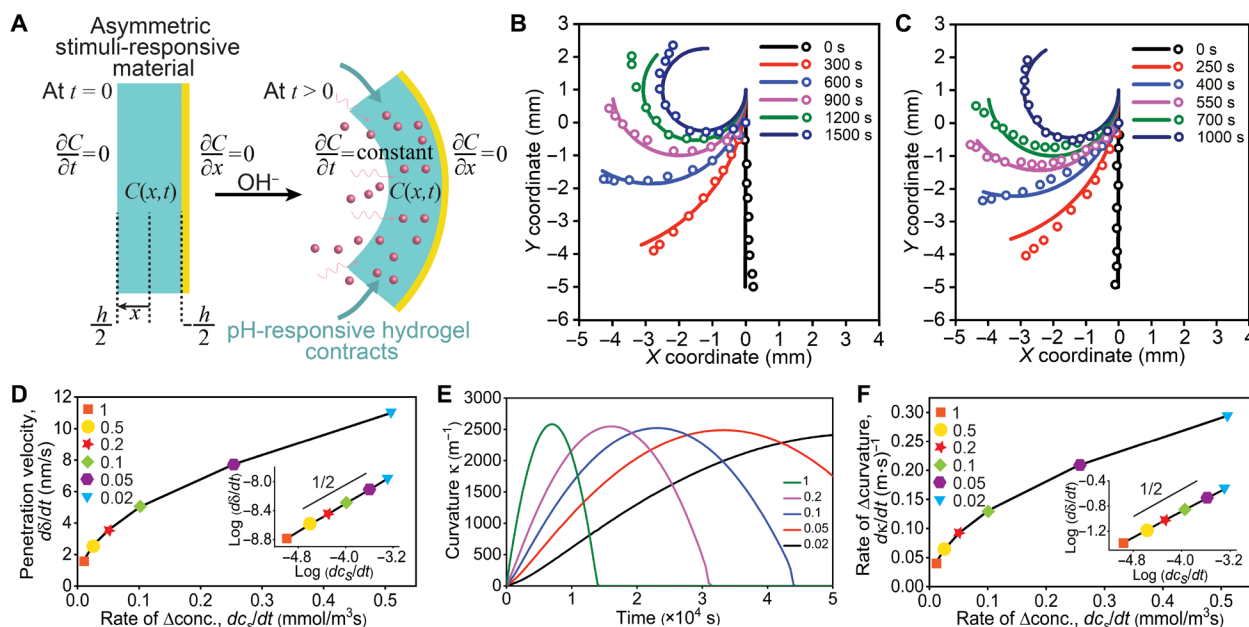


**Fig. 4. Modeling the bending of the asymmetric pH-responsive material based on the temporal derivative.** (A) Scheme illustrating the one-sided unsteady-state reaction diffusion of  $\text{OH}^-$  ions from the medium into the asymmetric pH-responsive material that caused the bending actuation. Bending of the asymmetric pH-responsive material at different times in a medium that changed from pH 7 to pH 11 in two ways: (B) a slower rate of injecting a pH 12 solution at 0.15 ml/min and (C) a higher rate of injecting a pH 12 solution at 0.25 ml/min. Numerical solutions of the modeling of the bending of the asymmetric pH-responsive material (solid lines) agree with the experimental data (open circles). (D) Plot of the velocity of penetration depth,  $\delta\delta/dt$ , versus the temporal derivative of the concentration of  $\text{OH}^-$  ions in the medium,  $dc_3/dt$ , derived from the numerical solution of the model for different normalized rates of change of concentration. Inset shows the plot in logarithmic scale with a slope of one-half. (E) Plots of the curvature,  $\kappa$ , of the asymmetric pH-responsive material with time derived from the model. The differently colored curves represent the trends for different temporal derivative of concentration of  $\text{OH}^-$  ions in the medium. The rates indicated in the legend are normalized with respect to the maximum temporal derivative of concentration by the injection of 0.25 ml/min of a pH 12 solution into the medium. (F) Plot of the initial rate of change of the curvature,  $d\kappa/dt$ , versus the temporal derivative,  $dc_3/dt$ , derived from the model for different normalized rates of change of concentration. Inset shows the plot in logarithmic scale with a slope of one-half. This plot thus conveniently serves as the calibration curve: Through quantifying the rate of bending of the asymmetric stimuli-responsive material at initial times experimentally, the temporal gradient of concentration in the medium can be determined via referring to this plot.

ammonium groups in the expanded pH-responsive hydrogel were deprotonated by the  $\text{OH}^-$  ions in the solution. Because the polymeric chains were no longer charged, the hydrogel contracted to its original state. The asymmetric contraction of the hydrogel due to the one-sided reaction diffusion of the  $\text{OH}^-$  ions caused the material to bend toward the uncoated side of the hydrogel. After ~20 min, the bending was so large that the asymmetric pH-responsive material curled and rolled onto itself. It bent faster when the increase in pH was larger, as shown by the experiment in which the medium was changed from deionized water to a pH 12 solution (Fig. 2B).

We further studied the performance of the asymmetric pH-responsive material by changing the pH gradually. Specifically, the pH of the deionized water was increased at a gradual linear rate of either 1 pH unit per 30 min or 1 pH unit per 10 min (see Materials and Methods for more details on the method of changing the pH linearly with time and fig. S4). Similarly, results showed that the asymmetric pH-responsive material bent in both cases, and a faster change in pH produced a faster rate of bending (Fig. 2, C and D). On the other hand, changes in the condition of the liquid medium may involve a linear change in the concentration of the chemical species (e.g.,  $\text{H}^+$  or  $\text{OH}^-$  ions) instead of the linear change in pH in many practical circumstances. Hence, we further performed experiments in which a basic solution (i.e., at pH 12) was injected into the deionized water at a constant flow rate of 0.15 or 0.25 ml/min (Fig. 2, E and F). Similar

trends of the bending were observed. In general, all these results showed that a larger increase in the concentration of the base in the medium led to a faster rate of bending, regardless of the way the concentration was increased (e.g., stepwise or gradual; see fig. S5 for a clear comparison of the bending with different conditions at the same time points).

For all our experiments, we observed that the asymmetric pH-responsive material straightened and became flat again after we stopped the change in pH of the medium [rightmost images of Fig. 2 (A and B)]. The time taken to become flat was relatively long; the reason was possibly that the transport of the  $\text{OH}^-$  ions into the pH-responsive hydrogel was highly limited after the material rolled onto itself compactly with the coated impermeable elastomer on the outside. As long as the pH did not change with time, the asymmetric pH-responsive material was always flat at equilibrium regardless of the magnitude of the pH, including pH 2 (i.e., the fully expanded state), pH 7, pH 10, pH 11, or pH 12 (i.e., the fully contracted state; Fig. 2G).

### Smart and adaptive asymmetric stimuli-responsive material

We examined the properties of the asymmetric pH-responsive material (Fig. 3A). It was able to change its size substantially at different pH (Fig. 3B). We found that it expanded in an acidic medium (pH 2)

and contracted in a basic medium (pH 12) reversibly for more than 15 cycles while maintaining the same sizes (fig. S6). Stimuli-responsive hydrogels can generally change their sizes reversibly for many cycles without any decrease in performance (32).

The coating of elastomer was highly adaptive. First, the elastomer was highly stretchable: It had a much smaller elastic modulus (i.e., 50 kPa; Fig. 3C) compared to the pH-responsive hydrogel (i.e., 800 kPa) and can stretch up to 980% of its original length without breaking (33). We found from scanning electron microscopy (SEM) that the thickness of the coating of elastomer was  $<1\ \mu\text{m}$  (Fig. 3D). Notably, we observed that the asymmetric pH-responsive material remained flat even when its length expanded by around two times at pH 2 from its unhydrated state. If the tension from stretching the layer of elastomer were substantial, it would have bent toward the side with the coating when expanded. The coating of elastomer thus had negligible mechanical influence over the material—the bending or flattening depended only on the stimuli-responsive hydrogel.

The coating of elastomer was impermeable. We observed that dye molecules were not able to diffuse through the asymmetric pH-responsive material coated with the elastomer even when it was expanded (Fig. 3E). However, the dye passed readily through the pH-responsive hydrogel when it was not coated with the layer of elastomer. We determined that the surface of the pH-responsive hydrogel coated with the elastomer was hydrophobic whether it was contracted or expanded (i.e., via measuring the contact angle of water in both these states; Fig. 3F). We analyzed both the surfaces of the slab of asymmetric pH-responsive material for both the expanded and contracted states (i.e., via freeze drying) by SEM (Fig. 3G). For the surface coated with the elastomer, no pores were observed for both the expanded and contracted states. In general, the surfaces coated with the elastomer of both the expanded and contracted states were similar from the images; hence, the coated layer seems adaptive and retains its properties at different states.

### Asymmetric glucose-responsive material

This approach is general because stimuli-responsive hydrogels can readily be fabricated to respond to many different types of stimuli. To demonstrate the generality of our method, we fabricated an asymmetric glucose-responsive material that consisted of a glucose-responsive hydrogel similarly coated asymmetrically with a layer of elastomer. Glucose monitoring and regulation in the human body are important for minimizing the adverse effects of the extreme levels of glucose (34). However, it is challenging to control the concentration of glucose because it can fluctuate unpredictably depending on many factors, including the habits of consumption (e.g., sweet foods), type of lifestyle, and many biological factors (35). Hence, there is a need to detect any rapid increase in the concentration of glucose (i.e., the temporal derivative) and control it pre-emptively before unhealthy levels are reached. We first determined that the glucose-responsive hydrogel changed its size continuously in the range of 0 to 500 mg/dl of glucose (i.e., the common range covered by devices for diabetic patients) (36). Similarly, we observed that the asymmetric glucose-responsive material bent when a solution containing glucose (500 mg/dl) was injected into the medium at a constant flow rate of 0.1 ml/min (Fig. 2H). When the glucose solution was injected at a higher rate of 0.3 ml/min, the asymmetric glucose-responsive material bent faster.

### Modeling the mechanism of analysis by the derivative

For understanding the fundamental mechanism of the process, we modeled the bending actuation of the asymmetric pH-responsive material due to the temporal derivative of the stimulus. The overall process involves the diffusion of the  $\text{OH}^-$  ions from the medium into the pH-responsive hydrogel, reaction of the  $\text{OH}^-$  ions with the protonated amine groups within the hydrogel, and nonhomogeneous contraction of the hydrogel (Fig. 4A). Because the length of the hydrogel (5 mm) is much larger than its thickness ( $\sim 160\ \mu\text{m}$ ), we assume that the reaction-diffusion process is only one-dimensional (1D) through the thickness of the hydrogel,  $x$ . The system of unsteady-state reaction-diffusion equations with respect to time,  $t$ , is shown in Eqs. 1 and 2 (section S2)

$$\frac{\partial c(x,t)}{\partial t} = D \frac{\partial^2 c(x,t)}{\partial x^2} + k_-(s_0 - s(x,t)) - k_+ s(x,t) c(x,t) \quad (1)$$

$$\frac{\partial s(x,t)}{\partial t} = k_-(s_0 - s(x,t)) - k_+ s(x,t) c(x,t) \quad (2)$$

$c$  and  $s$  represent the concentrations of the  $\text{OH}^-$  ions and the protonated amine groups, respectively.  $s_0$  is the concentration of the protonated amine groups in the hydrogel initially in deionized water.  $D$  is the diffusion coefficient of the  $\text{OH}^-$  ions in the pH-responsive hydrogel.  $k_+$  and  $k_-$  represent the forward and backward rate constants of the reaction, respectively. For this model, we applied two types of changes in concentration to the medium: pH 12 solution injected at a constant flow rate of 0.15 or 0.25 ml/min.

The contractile strain,  $\epsilon$ , can be modeled according to the logistic function  $\epsilon(c) = \epsilon_{\text{max}}(1 + K/c)^{-1}$ , where  $\epsilon_{\text{max}}$  is the maximum contractile strain and  $K$  is the mid-strain concentration. These two parameters were obtained by fitting the logistic function with the experimentally determined sizes of the asymmetric pH-responsive material at different pH at equilibrium (section S2 and fig. S7) (37). On the basis of this expression, the curvature,  $\kappa$ , of the bending of the asymmetric pH-responsive material with time can be obtained by integrating the moment of the strain across its thickness,  $h$ , according to Eq. 3

$$\kappa(t) = \frac{12 \epsilon_{\text{max}}}{h^3} \int_{-h/2}^{h/2} \left( \frac{x}{1 + K/c} \right) dx \quad (3)$$

After solving the equations numerically, the bending of the asymmetric pH-responsive material with time,  $\kappa(t)$ , derived from the model is found to be in good agreement with the experimental results for both rates of injection (Fig. 4, B and C). This agreement suggests that the fundamental mechanism by which the asymmetric pH-responsive material bends is due to the one-sided reaction-diffusion process of  $\text{OH}^-$  ions into the pH-responsive hydrogel coupled with the asymmetric contraction of the hydrogel.

We further examined the equations theoretically (section S3). First, we note that the deprotonation of the amine groups by the  $\text{OH}^-$  ions is an extremely fast reaction. This 1D diffusion-limited reaction of  $\text{OH}^-$  ions is characterized by a distinct reaction front. The penetration depth,  $\delta$ , of the reaction front, within which the reaction is completed, is an indicator of the amount of bending. Specifically, a larger  $\delta$  produces more bending for  $\delta < h/2$ . On the basis of our theoretical analysis of the equations, we found that the velocity of the penetration depth into the bulk of the hydrogel,

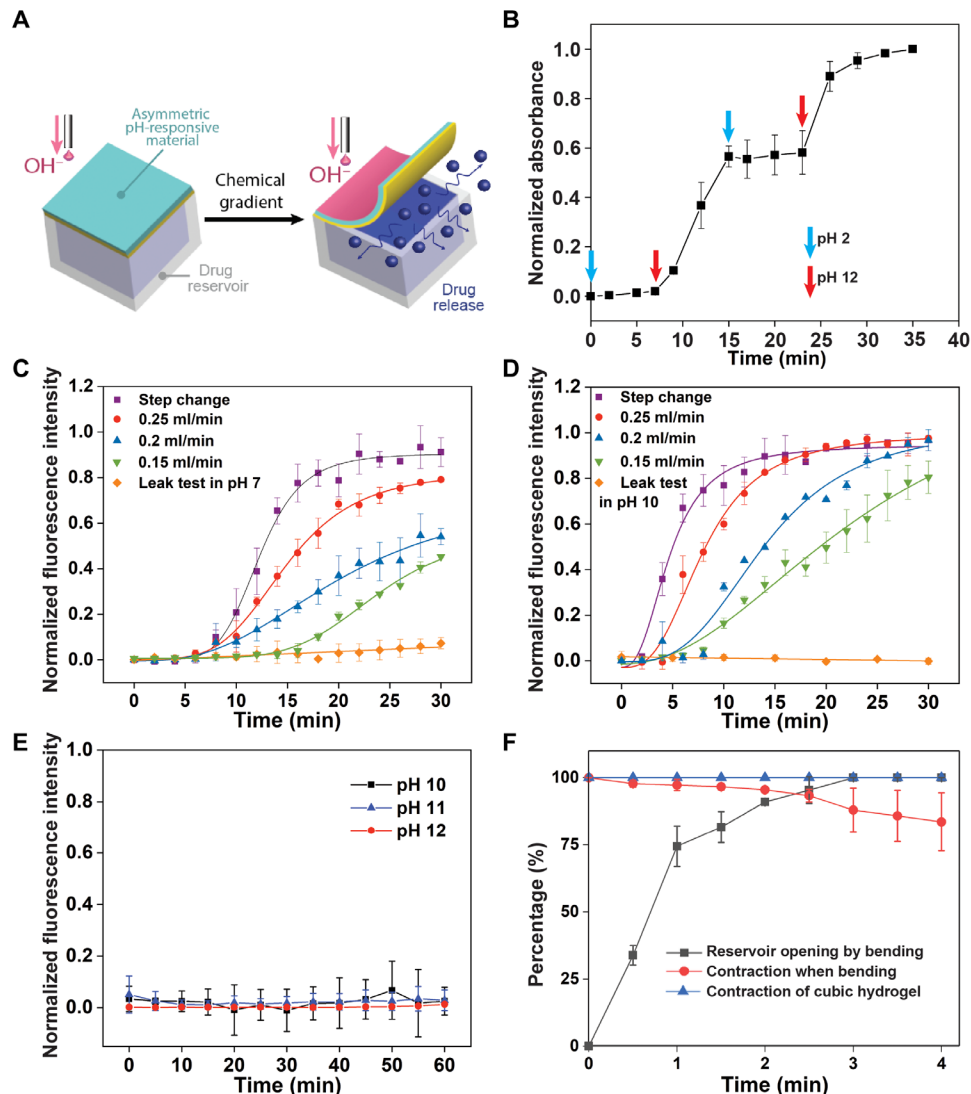


**Fig. 5. Derivative controller for controlled delivery.** (A) The smart tablet consists of a reservoir of drug and the asymmetric pH-responsive material that covers the reservoir. When the pH of the medium changes, the asymmetric pH-responsive material bends and releases the drug from the reservoir. (B) Reversible on-off controlled release. Fluorescent dye released in a pH 12 solution and was blocked from releasing in a pH 2 solution reversibly. Dye released when the pH of the medium was changed from (C) pH 7 to pH 11 or (D) pH 10 to pH 11.48. In both cases, the pH of the medium was increased in four ways: pH was changed rapidly (i.e., by injecting a basic solution at a very high flow rate of 25 ml/min; purple squares) or gradually by injecting a basic solution at a constant flow rate of 0.25 ml/min (i.e., 0.5  $\mu\text{M/s}$  for pH 7 to pH 11 and 1.5  $\mu\text{M/s}$  for pH 10 to pH 11.48; red circles), 0.2 ml/min (i.e., 0.4  $\mu\text{M/s}$  for pH 7 to pH 11 and 1.2  $\mu\text{M/s}$  for pH 10 to pH 11.48; blue triangles), or 0.15 ml/min (i.e., 0.3  $\mu\text{M/s}$  for pH 7 to pH 10 and 0.9  $\mu\text{M/s}$  for pH 10 to pH 11.48; green inverted triangles). pH of the medium was not changed (orange diamonds). (E) No release of the fluorescent dye when the pH of the medium (i.e., pH 10, 11, or 12) remained unchanged with time regardless of the magnitude of the pH. (F) Rates of response of the asymmetric pH-responsive material and a cubic piece of pH-responsive hydrogel.

$d\delta/dt$ , scales with the temporal derivative of the concentration of  $\text{OH}^-$  ions in the medium,  $dc_s/dt$ , according to  $d\delta/dt \sim \sqrt{dc_s/dt}$  (section S3). Numerical solution of the system of the unsteady-state reaction-diffusion equations validated this scaling relationship (Fig. 4D). For the bending actuation, we plotted the change in curvature,  $\kappa$ , with time for different temporal derivative,  $dc_s/dt$  (Fig. 4E; see fig. S8 for plot of curvature against the rate of change of concentration).  $\kappa$  initially increases as  $\delta$  increases with time. The curvature reaches a maximum value of  $\kappa_{\text{max}} = 3\epsilon_{\text{max}}/2h$  when  $\delta$  reaches half the thickness of the hydrogel (i.e.,  $\delta = h/2$ ). For  $\delta > h/2$ ,  $\kappa$  decreases and the asymmetric pH-responsive material straightens out. For the case when the penetration depth is small

(i.e.,  $\delta \ll h/2$ ), we found from our theoretical analysis that the rate of change of curvature scales directly with the temporal derivative according to  $d\kappa/dt = \sqrt{dc_s/dt}$ . This theoretical relationship is again verified by the numerical solution of the model (Fig. 4F).

In calculus, the temporal derivative is defined as the difference between the current and past levels of the stimulus with time. The unsteady-state reaction diffusion of molecules allows the asymmetric stimuli-responsive material to analyze the stimulus in a similar way. First, we note that the bending actuation is caused by the spatial difference in the concentration of the ions across the thickness of the pH-responsive hydrogel. On the other hand, the spatial concentration in the hydrogel is strongly related to the temporal change



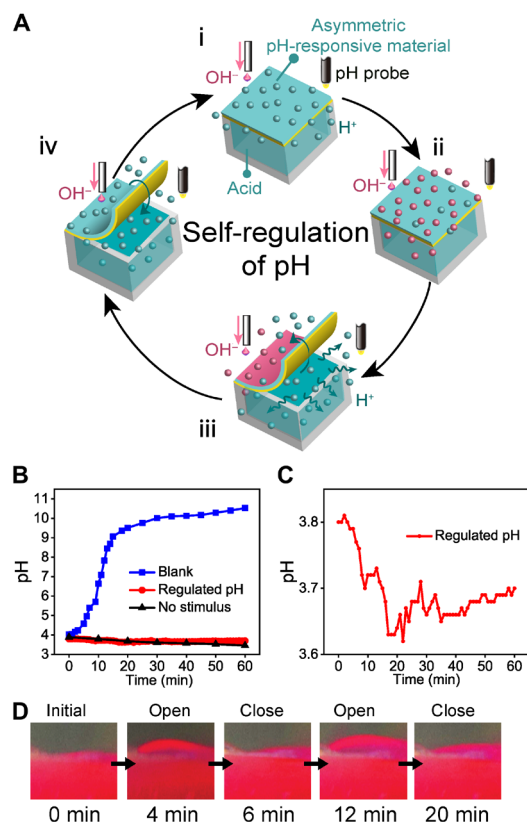


**Fig. 6. Derivative controller for self-regulation.** (A) Feedback mechanism for the self-regulation of pH of the medium by the controller with the asymmetric stimuli-responsive material. (B) The controller regulated the pH of the medium at around pH 4 even when a large disturbance (i.e., pH 12.2 solution injected at a flow rate of 0.15 ml/min or 0.5  $\mu$ M/s) was applied continuously for 60 min (red line). When the controller did not contain any concentrated acid in its reservoir, the pH of the medium increased due to the disturbance as expected (blue line). The leakage from the controller was observed to be negligible (black line). (C) Plot with an enlarged y axis of the red line shown in (B). (D) Experimental images showed that the asymmetric pH-responsive material opened and closed the reservoir repeatedly. The red color was due to the dye mixed with the concentrated acid in the reservoir.

in concentration in the medium: There is a general tendency of the concentration in the hydrogel close to the uncoated surface to be influenced by the recent concentrations of the medium, whereas the concentration deep into the bulk of the hydrogel tends to be influenced by the concentration of the medium at earlier times. Because of this relationship between the spatial concentration in the hydrogel and the temporal concentration in the medium, the bending of the asymmetric stimuli-responsive material thus involves the analysis of the differences between the current and past levels of the concentration in the medium continuously—in a way that is analogous to the calculation of the temporal derivative in calculus. A thin stimuli-responsive hydrogel corresponds to allowing the derivative to be determined over a small difference in time (i.e., an operation that corresponds to taking the limit with time).

### Controlled delivery based on the derivative

In addition to being a sensor, we showed that the bending actuation of the asymmetric stimuli-responsive material can be used for controlled delivery of drugs or chemicals—the control is based on the temporal derivative of concentration of the medium. We fabricated

a freestanding smart tablet (~mm) that consisted of a reservoir of dye (rhodamine B) and the asymmetric pH-responsive material (Fig. 5A). The slab of asymmetric pH-responsive material was adhered onto the tablet such that the surface of the elastomer covered the opening of the reservoir; thus, the impermeable elastomer served the additional function of preventing the dye from releasing from the reservoir. Only one end of the asymmetric pH-responsive material was adhered onto the tablet, while the other end was free to bend.

After fabrication, we first showed that the release of molecules from the reservoir could be switched on and off reversibly for flexible controlled release based on the condition (i.e., stimulus) of the surrounding medium. The smart tablet was initially (i.e., at  $t = 0$  min) immersed in a pH 2 medium; without a change in pH, no release of dye was observed (Fig. 5B). At time  $t = 7$  min, we changed the medium rapidly to pH 12. This sudden change in pH caused a large amount of dye to be released. At  $t = 15$  min, we changed the medium back to pH 2. This change caused the asymmetric pH-responsive material to flatten out and block the release of the dye. At  $t = 24$  min, we changed the medium back to pH 12 and observed that the dye was released again.

We determined that the smart tablet responded to the temporal derivative of the pH of the medium. Experimentally, we changed the pH of the medium from pH 7 to pH 11 at different rates. The fluorescent intensities of samples of the medium taken at regular time intervals showed that the dye molecules released whenever the pH changed (Fig. 5C). We found that a larger temporal derivative (i.e., due to a higher flow rate) corresponded to a faster rate of release of the dye. The responsiveness of the smart tablet was general and not restricted only to the change from pH 7 to pH 11. As a demonstration, we repeated the experiment, except that we changed the pH from 10 to 11.48 at different rates instead. Qualitatively similar results were obtained (Fig. 5D). These results demonstrated that the controller was able to produce generally similar trends of the response even when the starting pH values were very different; hence, the response of the controller was only dependent on the rate of change but not the absolute magnitude of the stimulus applied. In addition, we performed the control experiments in which the smart tablet was placed in the medium with different magnitudes of pH but without any change of pH with time (i.e., zero temporal derivative). Specifically, we immersed the smart tablet into a medium that was at pH 10, 11, or 12 and injected a solution of the same pH (i.e., at 0.2 ml/min) into the medium (i.e., for a fair comparison with the experiment in which the pH was changed by injecting a solution with a different pH). Results showed that there was no release of the dye regardless of the magnitude of the pH as long as it remained constant with time (Fig. 5E).

Because the detection and analysis were based on the temporal derivative, the smart tablet was able to provide a fast response under the influence of the stimulus. In most cases that involve stimuli-responsive hydrogel as the drug carrier for controlled release as reported in literature, the amount of release is usually directly proportional to the size of the hydrogel (i.e., not the derivative). Specifically, a common example from previous studies involves a stimuli-responsive hydrogel with a drug loaded in its bulk matrix in its expanded state. When the hydrogel contracts under the influence of the stimulus, the drug is squeezed out of the matrix and released to the surrounding medium. For comparing the speed of response, we fabricated the same pH-responsive hydrogel with exactly



the same volume as that used in our asymmetric pH-responsive material; however, it was cubic (i.e., not the flat thin piece of hydrogel used in the asymmetric pH-responsive material) and not coated with the elastomer. After fabrication, we repeated the same experiment as discussed in Fig. 2F for the asymmetric pH-responsive material: The cubic piece of hydrogel was initially immersed in deionized water (80 ml), and then a pH 12 solution was added gradually at a flow rate of 0.25 ml/min until the medium reached pH 11. Its size was monitored with respect to time. Our result showed that the cubic piece of pH-responsive hydrogel took a long time to fully contract: 240 min. For the first 4 min, the percentage of contraction of the hydrogel was completely negligible (blue triangles in Fig. 5F). In comparison, a significant amount of bending was observed for the asymmetric pH-responsive material within the first 4 min. This rapid bending allowed the reservoir to be mostly opened for releasing the molecules within 1 min and fully opened at around the first 3 min (black squares in Fig. 5F). On the other hand, we found that the overall percentage of contraction of the asymmetric pH-responsive material was relatively small (red circles in Fig. 5F). These results showed that the fast response of the asymmetric pH-responsive material was due to the very slight contraction on the side of the pH-responsive hydrogel that was exposed to the medium that, nevertheless, gave rise to a large amount of bending and release.

### Self-regulation based on the derivative

Besides controlled delivery, we showed that the device can be used as a controller for self-regulation of the concentration of a chemical in the medium. The controller consisted of the asymmetric pH-responsive material and a reservoir of concentrated acid mixed with a red dye for visualization [part (i) of Fig. 6A]. The controller was initially immersed in an aqueous medium of around pH 4. To investigate the self-regulating performance of the controller, we introduced a large disturbance to the medium by injecting a highly basic solution of pH 12.2 at a constant flow rate of 0.15 ml/min continuously for 60 min [part (ii) in Fig. 6A]. The disturbance caused the asymmetric pH-responsive material to bend and allowed the concentrated acid to be released from the reservoir [part (iii) in Fig. 6A]. The rapid drop in pH of the surrounding medium due to the release of the concentrated acid allowed the asymmetric pH-responsive material to flatten back again and block further release of the acid [part (iv) in Fig. 6A]. Our experimental results showed that this dynamic feedback mechanism between the bending of the asymmetric pH-responsive material and the medium allowed the pH of the medium to be controlled (red line of Fig. 6B). We performed two control experiments. The first control experiment involved a controller in which the reservoir did not contain any concentrated acid. In this case, the disturbance produced a large change in the pH of the medium as expected (blue line in Fig. 6B). The second control experiment involved the controller that contained the concentrated acid, but no basic solution was added to the medium as the disturbance. The leakage from the controller was observed to be negligible (black line in Fig. 6B).

A more detailed examination of the changes in pH with time showed that the self-regulation of pH (i.e., red line in Fig. 6B) involved repeated cycles of small amounts of increasing and decreasing pH of the medium (Fig. 6C). This oscillatory trend of the pH of the medium suggested that there were intermittent release and no release of the acid from the reservoir. A close observation of the asymmetric pH-responsive material showed that it did undergo

repeated cycles of small extents of bending and flattening for controlling the release of the acid from the reservoir (Fig. 6D). These dynamic responses from the asymmetric pH-responsive material allowed the pH of the medium to be regulated at an approximately constant pH with minimal fluctuations throughout the duration of the disturbance; thus, it achieved its function as a controller for self-regulation of the medium. The controller can be preprogrammed to control the pH of the medium at other desired set points via modifications such as changing the type of pH-responsive hydrogel used, the properties of the hydrogel (e.g., amount of cross-linking), and the concentration of the solution in the reservoir.

### DISCUSSION

Materials are generally perceived as “dumb” (e.g., a brick or wood). Even the class of smart materials (i.e., materials that are capable of interacting with their surroundings and providing a response) can only perform extremely primitive types of analytical operations (e.g., limited to simple logical operations such as half adders and half subtractors) despite recent rapid advances of the field (5, 38). The ultimate vision in current research is to create materials with highly developed analytical capabilities that one day can be considered “intelligent” (e.g., the capabilities of biological systems such as human beings and animals). These intelligent materials would be extremely useful owing to their potential capability and versatility to perform complex tasks autonomously for a wide range of applications (1). This manuscript describes a material that can perform the advanced mathematical operation of calculus—the temporal derivative—based on the signal that it receives from its surrounding. Notably, this approach illustrates that the temporal derivative can be determined without the use of a computer. This capability thus represents a substantial advancement from the extremely limited analytical functions of currently developed smart materials. Despite its advanced analytical ability, the material has an extremely simple structure: It consists of a piece of stimuli-responsive hydrogel coated asymmetrically with an adaptive and impermeable layer. This simple modification of the stimuli-responsive material is all that is needed to markedly change its ability to analyze the derivative unlike the elementary functions demonstrated by previously reported stimuli-responsive materials.

This study illustrates the fundamental possibility that materials can be tightly and directly associated with concepts of mathematics. First, the combination of the smart material and the physical-chemical process (i.e., the asymmetric unsteady-state reaction-diffusion process) interestingly allows for the operation of the transformation of variables: the continuous range of information in the temporal space (i.e., the temporal derivative of concentration) can be transformed directly to the spatial coordinates (i.e., spatial distribution of concentration within the stimuli-responsive hydrogel) for achieving the practically useful response (i.e., the bending actuation). This transformation of variables underlies the reason why it is physically possible for materials to analyze the derivative—a quantity in the temporal space. This unique capability of the transformation of the variable for analyzing the derivative is verified mechanistically by our model that agreed well with our experimental data. Our theoretical analysis further established the tight association of the material with mathematics: The rate of bending of the material scales with the square root of the temporal derivative. In addition, the mechanism established by the model indicates that as

the thickness of the stimuli-responsive hydrogel tends to infinitesimally small theoretically, the response from the asymmetric stimuli-responsive material is analogous to taking the limit of the change in concentration with time (i.e., refer to the section on modeling the mechanism of analyzing the derivative for a more detailed discussion); hence, this operation in the realms of materials science corresponds to the mathematical definition of the first temporal derivative. Many previous works have sought to perform mathematical functions from materials indirectly via the construction of logic gates (39, 40); however, a large number of elementary logic gates are typically needed for performing even simple mathematical operations. On the other hand, the association of materials directly with higher concepts of mathematics (e.g., the transformation of variables and analysis of the temporal derivative) as illustrated in this study is a powerful (i.e., effective and simple) approach that can potentially lead to the development of synthetic systems that can be considered intelligent in the future.

This ability to analyze and respond to the temporal derivative enables this class of asymmetric stimuli-responsive materials to serve as a derivative controller of processes. The derivative controller is a well-established device in the discipline of chemical engineering; it is currently being widely used in many industries (e.g., petrochemical and chemical) for the efficient regulation of manufacturing processes due to its ability to predict the future trend and provide fast corrective responses. However, these conventional controllers are complex (i.e., consist of many components including a computer), bulky, expensive, and difficult to operate. Hence, they cannot be used in many circumstances (e.g., for controlled drug delivery in a human body). We showed experimentally that this class of asymmetric stimuli-responsive material served effectively as a derivative controller for controlled delivery and self-regulation. We showed that the material provided a fast response based on its analysis of the derivative (e.g., when compared to the response rates by stimuli-responsive materials reported previously); hence, it realizes the same designed function of the industrial derivative controllers by engineers for the rapid stabilization of manufacturing processes. This class of material-based controllers has a number of important features. In particular, the structurally simple freestanding piece of asymmetric stimuli-responsive material simply integrates all the necessary elements of a controller within itself: the detection, analysis of the derivative, and response (i.e., bending actuation for controlled release). The operation is simple (i.e., the smart tablet only needs to be immersed in the medium for control), and the approach is general for different types of stimuli (e.g., pH and glucose). It does not require any additional energy input, equipment, or tethering to other components. Hence, these desirable features potentially allow this class of material-based controllers to be made widely accessible for a diverse range of applications, such as environmental and biomedical applications (e.g., drug delivery based on monitoring of glucose levels). Further studies will be needed to investigate its capabilities, optimize its performance, and combine this derivative controller with other types of controller in more detail. In general, this study demonstrates the approach and possibility to construct material-based systems (e.g., delivery systems or particles) that can control processes with similar functionality and efficiency as complex industrial controllers. Besides controlling processes, this asymmetric stimuli-responsive material can potentially also be used in any applications that require the analysis of the temporal derivative (e.g., sensors).

In addition, the result of this study highlights the general fundamental phenomenon that the bending actuation of stimuli-responsive materials generated by the analysis of the temporal derivative is capable of producing a fast response. Mechanistically, the reason why bending produces a fast response is because only a very slight contraction of one surface of the stimuli-responsive material is required to cause the large amount of bending. This result is useful for the design of synthetic machines (e.g., soft robots and actuators).

Coupled with the sheer simplicity of its structure, the asymmetric stimuli-responsive material can potentially be regarded as a basic materials module that can be incorporated easily into synthetic systems. This feature is well illustrated by biological systems: Basic structures that are similar to the asymmetric stimuli-responsive material are commonly found in nature for giving rise to mechanistically analogous operations. Examples from nature include the responsive materials that are coated to be impermeable on one side (e.g., the *H. bracteatum* that consists of hygroresponsive tissue coated with thicker waxy layer on one side as shown in Fig. 1F) or responsive materials that have sensors only on one side (e.g., *Drosera capensis* that consists of stress sensors on one side) (31, 41). Hence, as more synthetic systems with advanced functionalities are being developed, this class of asymmetric stimuli-responsive materials may also similarly be widely incorporated as a basic component within the synthetic systems for performing its unique advanced functions.

## MATERIALS AND METHODS

### Materials

2-(*N,N*-Dimethylamino)ethyl methacrylate (DMAEMA), 2-hydroxyethyl methacrylate (HEMA), ethylene glycol dimethacrylate (EGDMA), 2,2-dimethoxy-2-phenylacetophenone (DMPA), methacrylic acid (MAA), rhodamine B, sulfuric acid, and sodium hydroxide pellets were purchased from Sigma-Aldrich and were used as received. Acrylonitrile butadiene styrene (ABS) filaments and the 3D printer (UP! Plus 2) were purchased from Xpert Global Pte Ltd. (Singapore). The ABS filaments were the materials used in the 3D printer. A Sylgard 184 silicone elastomer kit was purchased from Dow Corning Co. (USA) and was used to make poly(dimethylsiloxane) (PDMS). Smooth-On Silc Pig blue-colored pigment was used to color the PDMS when required. Ultrapure water with a resistivity of 18 M $\Omega$ -cm was used in all experiments.

### Fabricating the PDMS mold for preparing the stimuli-responsive hydrogels

The fabrication of the PDMS mold used to prepare the stimuli-responsive hydrogels involved several steps as illustrated in fig. S1. The first step involved mixing the liquid monomer and cross-linker of PDMS in a 10:1 ratio with a small amount of the Silc Pig blue pigment. The mixture was mixed vigorously, poured into a petri dish, degassed for about 40 min, and baked in an oven for 1 hour at 75°C until it solidified. A strip of blue PDMS was cut and was adhered onto the bottom of a petri dish using double-sided tape as shown in fig. S1A. Copper foils (5 mm by 6 mm by 100  $\mu$ m) were inserted vertically into the strip of blue-colored PDMS, which served as the support for the copper foils. Subsequently, another volume of liquid monomer and cross-linker of PDMS were mixed in a 10:1 ratio, degassed, and poured into the petri dish until the copper foils were fully submerged in the liquid. The petri dish that contained the liquid mixture, the copper foils, and the blue-colored

strip of PDMS was then placed in an oven operated at 75°C for 2 hours. After polymerizing the PDMS, the strip of blue-colored PDMS and the copper foils were extracted. The open slits created by removing the copper foils on one surface of the PDMS were the molds for preparing the stimuli-responsive hydrogels.

### Preparing the pH-responsive hydrogel

HEMA [77.89 mole percent (mol %)], DMAEMA (19.53 mol %), DMPA (1.6 mol %) as the photoinitiator, and EGDMA (0.98 mol %) as the cross-linker were mixed thoroughly in a 5-ml Eppendorf tube using a vortex mixer. One milliliter of the mixture was then carefully injected into the open slits of the PDMS mold prepared as described in the previous paragraph. The PDMS mold containing the liquid mixture was subsequently placed under a 365-nm ultraviolet (UV) lamp (OmniCure S2000) for 15 min. After polymerization, the mold was cut open, and the thin slabs of pH-responsive hydrogel were extracted. This hydrogel was measured to have a thickness of 80  $\mu\text{m}$  by a Vernier caliper after polymerization.

### Preparing the glucose-responsive hydrogel

HEMA (79.8 mol %), MAA (17.2 mol %), EGDMA (1.7 mol %), and DMPA (1.3 mol %) were mixed in a 5-ml Eppendorf tube using a vortex mixer. A 100- $\mu\text{l}$  solution of this mixture was added into a tube containing 4 mg of glucose oxidase. Three microliters of catalase was also added to this mixture. The mixture was sonicated using an ultrasonicator (Elmasonic S 50 R, Elma Schmidbauer GmbH) to disperse the enzyme powder uniformly. The mixture was then injected into the open slits of the PDMS mold and cured under UV for 30 min. The slabs of glucose-responsive hydrogel were extracted from the PDMS mold and stored in a fridge at  $-18^{\circ}\text{C}$  before use. This glucose-responsive hydrogel changed its size continuously in the range of 0 to 500 mg/dl of glucose (i.e., the common range covered by the devices for people with diabetes).

### Fabricating the asymmetric stimuli-responsive material

After preparing the stimuli-responsive hydrogel as described in the previous paragraphs, it was coated with a layer of elastomer (i.e., Ecoflex™). The procedure involved first adhering the slabs of stimuli-responsive hydrogels (directly after polymerization) onto the bottom of a petri dish using two strips of double-sided tape as illustrated in fig. S2. Parts A and B of Ecoflex™ 00-50 were mixed in a 1:1 proportion and spin-coated onto the surface of the stimuli-responsive hydrogel at 5000 rpm for 1 min. The elastomer was cured for 4 hours. After curing, the stimuli-responsive hydrogel coated with the elastomer was extracted (i.e., cut out from the extra portions of the elastomer that spread after spin coating). The elastomer bonded onto the stimuli-responsive hydrogel tightly after curing. The liquid monomer of the elastomer probably penetrated into the porous surface of the stimuli-responsive hydrogel; after polymerizing the elastomer, the entanglement of the polymeric chains of the elastomer and hydrogel probably produced the tight bonding. Only the top surface of the stimuli-responsive hydrogel was coated with the elastomer; any elastomer at the bottom surface of the stimuli-responsive hydrogel (e.g., due to the flow of the liquid monomers of the elastomer into the void spaces created by the gap between the pieces of double-sided tape) was carefully scraped and removed using a pair of tweezers. This asymmetric pH-responsive material was then immersed in a pH 2 solution. After it fully expanded, asymmetric pH-responsive material was cut to lateral dimensions of 3 mm by 5 mm.

The layer of elastomer has negligible mechanical influence toward the bending or straightening of the asymmetric pH-responsive material. For example, after fabricating the asymmetric stimuli-responsive material, it was initially flat. We then placed it in a pH 2 solution. It expanded in the acidic solution and bent initially; subsequently, it became flat again. In this case, the elastomer was stretched readily and did not result in any permanent bending of the material even when it was fully expanded. When placed in a solution of pH 10 or more, the asymmetric pH-responsive material contracted. Again, we found that it was flat at steady state.

### Preparing the pH solutions

In this study, typical pH solutions of pH 2 ( $0.5 \times 10^{-2}$  M  $\text{H}_2\text{SO}_4$  solution), pH 10 ( $1 \times 10^{-4}$  M NaOH solution), pH 11 ( $1 \times 10^{-3}$  M NaOH solution), pH 12 ( $1 \times 10^{-2}$  M NaOH solution), and pH 12.2 ( $1.6 \times 10^{-2}$  M NaOH solution) were prepared by adding either acidic or alkaline (i.e.,  $\text{H}_2\text{SO}_4$  or NaOH) solution dropwise into a bottle of deionized water until the pH of the solution was adjusted to the required value. A pH probe (Mettler Toledo, SevenCompact S220) was placed in the bottle to read the pH value. The bottle was placed on a magnetic stirrer (WIGGENS hotplate stirrer WH220 plus, Germany) and stirred continuously during the process of adding the acid or alkaline solution dropwise. Once the measurement of the pH stabilized, the bottle was capped and sealed using a parafilm before use.

### Measuring the contraction ratio of the asymmetric stimuli-responsive material

For measuring the amount of contraction at equilibrium at different pH, the piece of asymmetric pH-responsive material was first placed in a petri dish containing a pH 2 solution and allowed to expand. The length,  $L_{\text{expanded}}$ , of the expanded asymmetric pH-responsive material was measured using a stereomicroscope (Leica DMS 1000). It was then washed thoroughly using deionized water to remove the acid in the material and placed in a dish containing the solution of a specific pH. After placing the material in the solution, the petri dish was sealed using parafilm (to prevent any disturbance on the pH from the surrounding). The length of the asymmetric pH-responsive material at equilibrium,  $L$ , was measured after immersing it in the solution of a specific pH for 6 hours (Fig. 3A). The contraction ratio of the asymmetric pH-responsive material at the specific pH is defined as  $L/L_{\text{expanded}}$ .

### Characterization of the bending of the asymmetric pH-responsive material

The asymmetric pH-responsive material was first soaked in deionized water ( $\sim\text{pH}$  5.4). It remained flat (i.e., no bending was observed) after soaking in deionized water at equilibrium. For performing the first set of experiments (i.e., observing the bending of the material), we changed the pH of the solution rapidly by removing the asymmetric pH-responsive material from the deionized water and immersing it in either a pH 11 or pH 12 solution. It was immersed by clamping it vertically with a pair of tweezers. Time-lapse images of the asymmetric pH-responsive material were captured at 30-s time intervals.

To investigate the bending of the asymmetric pH-responsive material with the linear changes of pH at different rates, the asymmetric pH-responsive material was immersed in a glass beaker filled with 50 ml of water at pH 7. Four basic solutions were prepared with different pH separately: 5 ml of pH 9 solution, 5.5 ml of pH 10

solution, 6.05 ml of pH 11 solution, and 6.655 ml of pH 12 solution. These solutions were stored in 10-ml syringes separately. They were injected into the glass beaker with syringe pumps (KD Scientific Legato 210) via 20-cm-long polystyrene tubes with an inner diameter of 1 mm. One end of the tube was connected to the needle of the syringe, while the other end was submerged in the glass beaker filled with the aqueous medium. The tube was prefilled with the basic solution with the same pH as the solution in the syringe. The total amount of solution in the syringe and the tube was the volume stated above for each solution. The syringe pump was preprogrammed to inject the basic solution so that there was a linear change in pH in the medium in the glass beaker; that is, the programming took into account the logarithmic relationship between the concentration of the  $\text{OH}^-$  ions and pH. Specifically, the program consisted of pumping out many (i.e., 30) short but constant injections of varying flow rates. The flow rates specified in the program were determined by the logarithmic relationship between the concentration of the  $\text{OH}^-$  ions and pH. The four basic solutions were pumped (with these preprogrammed flow rates) sequentially, starting from the solution with lowest pH to the solution with the highest pH. The injection of the solution from each syringe was used to increase the pH of the solution by 1 pH unit; hence, the four solutions in the syringes increased the pH of the solution by 4 pH units from pH 7 to pH 11. To prevent any disruptions between the pumping of the solutions from one syringe to another, two syringe pumps were used; they were coordinated so that when the injection of one pump stopped, the other began immediately. The polystyrene tubes were needed: Without the use of the tubes, droplets (due to surface tension) usually formed at the tip of the needles and did not drop into the solution until they were sufficiently large, thus causing the pH of the medium to spike abruptly when the droplet did fall into the medium. The medium in the glass beaker was stirred continuously throughout the experiment to ensure homogeneous mixing. The whole experiment was done in a  $\text{N}_2$ -protected environment to minimize the fluctuations of pH due to the surrounding atmosphere (e.g., by dissolved  $\text{CO}_2$ ). Time-lapse images of the bending of the material were captured every 30 s.

In another experiment, the pH of the solution was changed gradually instead of the stepwise manner. In this case, the asymmetric pH-responsive material was clamped vertically and initially immersed in 80 ml of deionized water. pH 12 solution was added gradually at a flow rate of 0.15 or 0.25 ml/min using a syringe pump (KD Scientific, Legato 100) until the pH of the solution finally reached pH 11. The solution was stirred gently (at 150 rpm) so that the convective currents due to the stirring did not disturb the asymmetric pH-responsive material. Time-lapse images of the bending of the material were captured every 30 s.

### Characterization of the bending of the asymmetric glucose-responsive material

The asymmetric glucose-responsive material (that consisted of the glucose-responsive hydrogel coated with a layer of elastomer on one surface) was first expanded in pH 12 and cut to the lateral dimensions of 3 mm by 5 mm. It was then clamped vertically by a pair of tweezers and immersed in a beaker containing 80 ml of deionized water at 37°C. The temperature was maintained at 37°C throughout the experiment. The solution in the beaker was stirred at 150 rpm. Subsequently, 30 ml of glucose solution (500 mg/dl) was injected into the beaker at a rate of 0.1 or 0.3 ml/min using a syringe pump.

Time-lapse images of the asymmetric glucose-responsive material were captured every 30 s.

### Analysis by scanning electron microscopy

SEM (JSM-5600LV, JEOL, Japan) was used to observe the morphology of the asymmetric pH-responsive material. The material was first either expanded in pH 2 or contracted in pH 12. It was then cooled overnight in a  $-21^\circ\text{C}$  freezer and freeze-dried (FreeZone 4.5 Plus, Labconco, USA) for 6 hours. Both the hydrogel side and the elastomer side of the asymmetric pH-responsive material were observed using SEM for the expanded and contracted states. Platinum was sputter-coated onto the freeze-dried hydrogels using a platinum sputter coater (Cressington 208HR, Cressington Scientific Instruments, UK). The coating was performed at  $5 \times 10^{-2}$  bar vacuum and 20-mA current for 90 s. The materials were then fixed to a double-sided carbon tape attached to an aluminum stub and imaged at 15-kV potential. The cross section of the asymmetric pH-responsive material was imaged by placing it on a cross-section stub.

### Wettability of the surface of the asymmetric pH-responsive material

The contact angle of water was measured for the elastomer side of the asymmetric pH-responsive material. The material was first either expanded in pH 2 or contracted in pH 12. A droplet of deionized water (4  $\mu\text{l}$ ) was then placed on the surface of the material coated with the layer of elastomer. An image of the droplet was taken using a Nikon D5300 camera fitted with an AF-S Micro-NIKKOR 105-mm lens (Nikon, Japan). The contact angle of water was measured from the image using Photoshop (Adobe).

### Elastic moduli of the elastomer and stimuli-responsive hydrogel

The stress-versus-strain curve was recorded using an Instron 5542 Single Testing Column System. The elastic moduli were calculated by taking the gradient at the linear region of the curve (i.e., at the beginning of the curve) at which Hooke's law is obeyed ( $\sim 10$  to 30% tensile strain).

### Testing the permeability of the asymmetric pH-responsive material

The asymmetric pH-responsive material was initially expanded in a pH 2 solution. It was then used in a two-chamber experimental setup for studying the permeability of the asymmetric pH-responsive material (Fig. 3E). The two-chamber setup consisted of a petri dish with a separator in the middle of the dish for creating the two chambers of liquid on either side of the separator. The separator consisted of two glass slides and the asymmetric pH-responsive material. Each of the two pieces of glass slides was first adhered (i.e., with New Orland Adhesive 63) to one side of the boundary of the petri dish as shown in Fig. 3E. The asymmetric pH-responsive material was then adhered to the two pieces of glass slide such that it was right in the center of the petri dish. In this way, the separator that consisted of the glass slides and the asymmetric pH-responsive material separated the petri dish into two chambers. The surface of the pH-responsive hydrogel faced one of the chambers, whereas the surface coated with the layer of elastomer faced the other chamber. For the chamber that the pH-responsive hydrogel faced, we filled it with a pH 2 solution to keep the hydrogel in its expanded state. For the chamber that the elastomer faced, we filled it with a dye (i.e.,



Orange G) solution. The setup was monitored for 24 hours. No diffusion of dye across the asymmetric pH-responsive material to the other chamber was observed even when the hydrogel was at its expanded state. On the other hand, dye passed through readily for the case when the pH-responsive hydrogel was not coated with the layer of elastomer.

### Testing the reversibility of the changes in size of the hydrogel

After fabricating the pH-responsive hydrogel, it was expanded in a pH 2 solution. The hydrogel was then cut into dimensions of 5 mm by 2 mm by 0.16 mm while it was in the expanded state. The longest dimension of the pH-responsive hydrogel (i.e., 5 mm) was defined as the expanded length,  $L_{\text{expanded}}$ . Subsequently, the hydrogel was contracted in a pH 12 solution for 8 hours to ensure that the hydrogel was fully contracted. The longest dimension of the pH-responsive hydrogel at equilibrium,  $L$ , was measured using a stereomicroscope (Leica DMS 1000). The hydrogel was then expanded fully in a pH 12 solution for 8 hours; its dimension equilibrium was again measured. The cycles were repeated for 15 times. The contraction ratio of the hydrogel at different pH was calculated by the formula  $L/L_{\text{expanded}}$ .

### Fabrication of the smart tablet for controlled delivery

The smart tablet consisted of a reservoir containing a dye solution and the asymmetric pH-responsive material that controlled the release of the dye. The smart tablet was fabricated by first printing a rectangular block of polymer (ABS) of dimensions 2 mm by 1 mm by 2 mm using a 3D printer as the template for the reservoir. This block of ABS was then adhered onto the bottom of a petri dish with double-sided tape. Prepolymer liquid PDMS was poured into the petri dish and was cured at 75°C overnight. After curing, the polymerized PDMS was separated from the petri dish, and the block of ABS was removed from the PDMS. The cavity left behind by the block of ABS in the PDMS served as the reservoir. The solid PDMS was cut into dimensions of 9 mm by 5 mm by 3 mm. A solution of rhodamine B dye was prepared by mixing 0.105 g of the dye in 7 ml of deionized water; it was then filled into the reservoir to the brim. In a separate step, the asymmetric pH-responsive material in the expanded state was cut to a size of 5 mm by 3 mm. The materials were then soaked in a solution of specific pH, depending on the type of test performed (as stated in the next section on testing the tablet). It was then placed over the reservoir such that the impermeable elastomer was in contact with the dye solution and fully covered the top opening (2 mm by 1 mm) of the reservoir. A cleaned thin layer of PDMS was used to wrap and secure one end of the asymmetric pH-responsive material (i.e., the extra length of the material that was not covering the opening) onto the solid PDMS.

### Testing the smart tablet for controlled delivery

After fabrication, the smart tablet was immersed in a (100 ml) beaker filled with 80 ml of deionized water or a solution of a required pH. The smart tablet was placed on top of a block of ABS with a height of 3 cm. The liquid was stirred at 450 rpm using a cylindrical magnetic pellet of 2 cm length and 6 mm diameter at the bottom of the beaker. For one demonstration, the asymmetric pH-responsive material that was attached on the smart tablet was presoaked in a pH 7 solution. Subsequently, the pH of the solution was changed either in a stepwise or gradual manner from pH 7 to pH 11. For the

stepwise change in pH, the change was conducted by injecting pH 12 solution at high flow rate of 25 ml/min directly into the beaker until the medium became pH 11. For the gradual increase in pH, a syringe pump (KD Scientific, Legato 100, USA) was used to add a total of 8 ml of pH 12 solution at a specific flow rate (i.e., 0.15, 0.2, or 0.25 ml/min) into the solution until the medium became pH 11. A pH probe (Mettler Toledo Seven Multi, Switzerland) was placed in the beaker to monitor the pH in real time. A liquid sample of 250  $\mu$ l was collected every 2 min until the entire reservoir of dye was released completely. The fluorescent intensities of the samples were analyzed. For establishing the calibration curve, the fluorescent intensities of a series of samples with known concentrations of the dye were measured (see fig. S9). Calculation based on the calibration plot showed that the final total amount of the dye in the solution after all the dye was fully released was approximately equal to the total amount of the dye in the reservoir of the controller initially.

Another demonstration involved changing the medium from pH 10 to pH 11.48. In this case, the asymmetric pH-responsive material that was attached on the smart tablet was presoaked in a pH 10 solution. The pH of the solution was then changed in either a stepwise or a gradual manner from pH 10 to pH 11.48 by injecting a pH 12.48 solution at different flow rates (i.e., 0.15, 0.2, 0.25, or 25 ml/min).

The smart tablet was tested for whether it leaked or not when there was no change in pH of the solution (i.e., zero temporal derivative). The asymmetric pH-responsive material was first presoaked in a solution of a specific pH (i.e., pH 10, 11, or 12). It was then attached to the smart tablet that was filled with dye. Subsequently, this smart tablet was immersed into a solution that contained the same pH that was used to presoak the asymmetric pH-responsive material. For this control experiment, the solution of the same pH was pumped into the beaker at a flow rate of 0.2 ml/min. The liquid (250  $\mu$ l) was sampled from the beaker every 5 min. We observed negligible leakage of the dye from the smart tablet for all the pH tested (i.e., 10, 11, or 12).

### Determining the reversible on-off release of the controller

The asymmetric pH-responsive material was first presoaked in a pH 2 solution and attached onto the reservoir for fabricating the smart tablet. This smart tablet was then immersed in a pH 2 solution. For determining the reversible on-off controlled release of the controller, the pH of the solution was first changed to pH 12 by adding 2.5 M NaOH solution dropwise. Subsequently, the pH of the solution was changed back to pH 2 by adding a concentrated  $\text{H}_2\text{SO}_4$  solution in dropwise manner. The pH of the solution was monitored using a pH probe throughout the experiment. A sample of the solution was taken every minute. The sample was analyzed by UV-visible (UV-vis) (Shimadzu UV-1800 UV-vis scanning spectrophotometer) and poured back into the original beaker immediately after every analysis to ensure that the concentration of the medium was not changed.

### Comparing response rate with cubic hydrogel

For fabricating the cubic pH-responsive hydrogel, 77.89 mol % HEMA, 19.53 mol % DMAEMA, 1.6 mol % DMPA as the photoinitiator, and 0.98 mol % EGDMA as the cross-linker were first mixed in a 5-ml Eppendorf tube thoroughly using a vortex mixer. The mixture was then carefully injected into a PDMS mold with a cubic cavity (i.e., dimensions of 0.5 cm by 0.5 cm by 0.5 cm) until the

cavity was completely filled. The PDMS mold containing the liquid mixture was subsequently polymerized by a 365-nm UV lamp. After polymerization, the pH-responsive hydrogel was extracted from the mold. It was then immersed in a pH 2 solution for approximately 10 hours to fully expand the cubic hydrogel. This large expanded cubic hydrogel was then cut into smaller cubes with sides of 1.34 mm. The volume of each of these cubic hydrogels was equal to the flat thin piece of pH-responsive hydrogel used in the asymmetric pH-responsive material in the expanded state.

For comparing the rates of response, the asymmetric pH-responsive material and the cubic pH-responsive hydrogel were each clamped vertically and immersed in 80 ml of deionized water separately. pH 12 solution was added gradually at a flow rate of 0.25 ml/min using a syringe pump (KD Scientific, Legato 100) until the pH of the solutions reached pH 11. Time-lapse images of the bending of the asymmetric pH-responsive material and the contraction of the cubic pH-responsive hydrogel were captured at every 30 s. The images were analyzed by Photoshop (Adobe).

### Fluorescence measurement

The sample (250  $\mu$ l) was loaded into the black polystyrene flat-bottomed 96-well plates (Corning Costar), and the fluorescence reading was read at excitation/emission wavelengths of 553/627 nm using a microplate reader (Tecan Infinite M200 Pro, Switzerland).

### Self-regulation using the pH-responsive controller

The controller was the same as the smart tablet, except that its reservoir was filled with a concentrated solution of (98%) sulfuric acid mixed with 2% rhodamine B instead. The asymmetric pH-responsive material was presoaked in pH 4 before attaching onto the controller. The controller was then immersed into a beaker filled with 80 ml of a pH 4 solution. A basic solution of pH 12.2 was added into the solution at a flow rate of 0.15 ml/min by a syringe pump via an injection tube as the disturbance. The injection tube was positioned close to the controller. Specifically, it was placed 5 mm vertically above the asymmetric pH-responsive material and 4 mm away from the edge of the asymmetric pH-responsive material (i.e., the side at which the material was adhered to the controller) in the horizontal direction. A pH probe was immersed in the solution for monitoring the pH. To minimize the disturbance caused by the injection of the basic solution onto the pH probe, the pH probe was placed on the opposite side of the controller with respect to the injection tube. Specifically, it was 5 mm vertically above and 5 mm away horizontally from the asymmetric pH-responsive material (i.e., the side of the material that was not adhered and free to bend). The controller can be preprogrammed to control the pH of the medium at different set points via modifications such as changing the type of pH-responsive hydrogel used, the properties of the hydrogel (e.g., amount of cross-linking), and the concentration of the solution in the reservoir.

### SUPPLEMENTARY MATERIALS

Supplementary material for this article is available at <http://advances.sciencemag.org/cgi/content/full/7/14/eabe5698/DC1>

### REFERENCES AND NOTES

- X. Zhang, L. Chen, K. H. Lim, S. Gonuguntla, K. W. Lim, D. Pranantyo, W. P. Yong, W. J. T. Yam, Z. Low, W. J. Teo, H. P. Nien, Q. W. Loh, S. Soh, The pathway to intelligence: Using stimuli-responsive materials as building blocks for constructing smart and functional systems. *Adv. Mater.* **31**, 1804540 (2019).
- M. A. C. Stuart, W. T. S. Huck, J. Genzer, M. Müller, C. Ober, M. Stamm, G. B. Sukhorukov, I. Szleifer, V. V. Tsukruk, M. Urban, F. Winnik, S. Zauscher, I. Luzinov, S. Minko, Emerging applications of stimuli-responsive polymer materials. *Nat. Mater.* **9**, 101–113 (2010).
- D. E. Seborg, D. A. Mellichamp, T. F. Edgar, F. J. Doyle III, *Process Dynamics and Control* (John Wiley & Sons, 2010).
- D. Schmaljohann, Thermo- and pH-responsive polymers in drug delivery. *Adv. Drug Deliv. Rev.* **58**, 1655–1670 (2006).
- X. Yan, F. Wang, B. Zheng, F. Huang, Stimuli-responsive supramolecular polymeric materials. *Chem. Soc. Rev.* **41**, 6042–6065 (2012).
- P. Theato, B. S. Sumerlin, R. K. O'Reilly, T. H. Epps III, Stimuli responsive materials. *Chem. Soc. Rev.* **42**, 7055–7056 (2013).
- X. Huang, C. S. Brazel, On the importance and mechanisms of burst release in matrix-controlled drug delivery systems. *J. Control. Release* **73**, 121–136 (2001).
- G. D. Kang, S. H. Cheon, S.-C. Song, Controlled release of doxorubicin from thermosensitive poly(organophosphazene) hydrogels. *Int. J. Pharm.* **319**, 29–36 (2006).
- K. E. Broaders, S. J. Pastine, S. Grandhe, J. M. Fréchet, Acid-degradable solid-walled microcapsules for pH-responsive burst-release drug delivery. *Chem. Commun.* **47**, 665–667 (2011).
- J. P. Goertz, K. C. DeMella, B. R. Thompson, I. M. White, S. R. Raghavan, Responsive capsules that enable hermetic encapsulation of contents and their thermally triggered burst-release. *Mater. Horiz.* **6**, 1238–1243 (2019).
- Y. Sun, S. Soh, Printing tablets with fully customizable release profiles for personalized medicine. *Adv. Mater.* **27**, 7847–7853 (2015).
- A. Matsumoto, T. Ishii, J. Nishida, H. Matsumoto, K. Kataoka, Y. Miyahara, A synthetic approach toward a self-regulated insulin delivery system. *Angew. Chem. Int. Ed.* **51**, 2124–2128 (2012).
- J. Wang, Y. Ye, J. Yu, A. R. Kahkoska, X. Zhang, C. Wang, W. Sun, R. D. Corder, Z. Chen, S. A. Khan, J. B. Buse, Z. Gu, Core-shell microneedle gel for self-regulated insulin delivery. *ACS Nano* **12**, 2466–2473 (2018).
- S. Angelos, Y.-W. Yang, N. M. Khashab, J. F. Stoddart, J. I. Zink, Dual-controlled nanoparticles exhibiting AND logic. *J. Am. Chem. Soc.* **131**, 11344–11346 (2009).
- S. Erbas-Cakmak, S. Kolemen, A. C. Sedgwick, T. Gunnlaugsson, T. D. James, J. Yoon, E. U. Akkaya, Molecular logic gates: The past, present and future. *Chem. Soc. Rev.* **47**, 2228–2248 (2018).
- H. Komatsu, S. Matsumoto, S. I. Tamaru, K. Kaneko, M. Ikeda, I. Hamachi, Supramolecular hydrogel exhibiting four basic logic gate functions to fine-tune substance release. *J. Am. Chem. Soc.* **131**, 5580–5585 (2009).
- L. Qian, E. Winfree, J. Bruck, Neural network computation with DNA strand displacement cascades. *Nature* **475**, 368–372 (2011).
- X. Zhang, S. Soh, Performing logical operations with stimuli-responsive building blocks. *Adv. Mater.* **29**, 1606483 (2017).
- H. Che, B. C. Buddingh', J. C. M. van Hest, Self-regulated and temporal control of a "breathing" microgel mediated by enzymatic reaction. *Angew. Chem. Int. Ed.* **56**, 12581–12585 (2017).
- H. Che, S. Cao, J. C. M. van Hest, Feedback-induced temporal control of "breathing" polymersomes to create self-adaptive nanoreactors. *J. Am. Chem. Soc.* **140**, 5356–5359 (2018).
- J. Cui, D. Daniel, A. Grinthal, K. Lin, J. Aizenberg, Dynamic polymer systems with self-regulated secretion for the control of surface properties and material healing. *Nat. Mater.* **14**, 790–795 (2015).
- X. He, M. Aizenberg, O. Kuksenok, L. D. Zarzar, A. Shastri, A. C. Balazs, J. Aizenberg, Synthetic homeostatic materials with chemo-mechano-chemical self-regulation. *Nature* **487**, 214–218 (2012).
- Z. Jiang, R. J. P. Sanchez, I. Blakey, A. K. Whittaker, 3D shape change of multi-responsive hydrogels based on a light-programmed gradient in volume phase transition. *Chem. Commun.* **54**, 10909–10912 (2018).
- R. Luo, J. Wu, N.-D. Dinh, C.-H. Chen, Gradient porous elastic hydrogels with shape-memory property and anisotropic responses for programmable locomotion. *Adv. Funct. Mater.* **25**, 7272–7279 (2015).
- Y. Klein, E. Efrati, E. Sharon, Shaping of elastic sheets by prescription of non-Euclidean metrics. *Science* **315**, 1116–1120 (2007).
- T. Xie, J. Li, Q. Zhao, Hidden thermoreversible actuation behavior of Nafion and its morphological origin. *Macromolecules* **47**, 1085–1089 (2014).
- Y. Zhong, F. Zhang, M. Wang, C. J. Gardner, G. Kim, Y. Liu, J. Leng, S. Jin, R. Chen, Reversible humidity sensitive clothing for personal thermoregulation. *Sci. Rep.* **7**, 44208 (2017).
- N. Bassik, B. T. Abebe, K. E. Laffin, D. H. Gracias, Photolithographically patterned smart hydrogel based bilayer actuators. *Polymer* **51**, 6093–6098 (2010).
- Z. Hu, X. Zhang, Y. Li, Synthesis and application of modulated polymer gels. *Science* **269**, 525–527 (1995).

30. T. S. Shim, S.-H. Kim, C.-J. Heo, H. C. Jeon, S.-M. Yang, Controlled origami folding of hydrogel bilayers with sustained reversibility for robust microcarriers. *Angew. Chem. Int. Ed.* **51**, 1420–1423 (2012).
31. D. Borowska-Wykręt, A. Rypień, M. Dulski, M. Grelowski, R. Wrzalił, D. Kwiatkowska, Gradient of structural traits drives hygroscopic movements of scarious bracts surrounding *Helichrysum bracteatum* capitulum. *Ann. Bot.* **119**, 1365–1383 (2017).
32. X. Huang, Y. Sun, S. Soh, Stimuli-responsive surfaces for tunable and reversible control of wettability. *Adv. Mater.* **27**, 4062–4068 (2015).
33. Y. Fouillet, C. Parent, G. Groppler, L. Davoust, J. L. Achard, F. Revol-Cavalier, N. Verplanck, Stretchable material for microfluidic applications. *Proceedings* **1**, 501 (2017).
34. M. Elsherif, M. U. Hassan, A. K. Yetisen, H. Butt, Wearable contact lens biosensors for continuous glucose monitoring using smartphones. *ACS Nano* **12**, 5452–5462 (2018).
35. J. Wang, Z. Wang, J. Yu, A. R. Kahkoska, J. B. Buse, Z. Gu, Glucose-responsive insulin and delivery systems: Innovation and translation. *Adv. Mater.* **32**, 1902004 (2020).
36. A. Heller, B. Feldman, Electrochemical glucose sensors and their applications in diabetes management. *Chem. Rev.* **108**, 2482–2505 (2008).
37. B. Zhao, J. S. Moore, Fast pH- and ionic strength-responsive hydrogels in microchannels. *Langmuir* **17**, 4758–4763 (2001).
38. L. Zhai, Stimuli-responsive polymer films. *Chem. Soc. Rev.* **42**, 7148–7160 (2013).
39. S. Uchiyama, N. Kawai, A. P. de Silva, K. Iwai, Fluorescent polymeric AND logic gate with temperature and pH as inputs. *J. Am. Chem. Soc.* **126**, 3032–3033 (2004).
40. D. Liu, W. Chen, K. Sun, K. Deng, W. Zhang, Z. Wang, X. Jiang, Resettable, multi-readout logic gates based on controllably reversible aggregation of gold nanoparticles. *Angew. Chem. Int. Ed.* **50**, 4103–4107 (2011).
41. M. Krausko, Z. Perutka, M. Šebela, O. Šamajová, J. Šamaj, O. Novák, A. Pavlovič, The role of electrical and jasmonate signalling in the recognition of captured prey in the carnivorous sundew plant *Drosera capensis*. *New Phytol.* **213**, 1818–1835 (2017).
42. H. Yuk, T. Zhang, G. A. Parada, X. Liu, X. Zhao, Skin-inspired hydrogel–elastomer hybrids with robust interfaces and functional microstructures. *Nat. Commun.* **7**, 12028 (2016).
43. S. H. Kim, S. Jung, I. S. Yoon, C. Lee, Y. Oh, J.-M. Hong, Ultrastretchable conductor fabricated on skin-like hydrogel-elastomer hybrid substrates for skin electronics. *Adv. Mater.* **30**, 1800109 (2018).
44. A. Roointan, J. Farzanfar, S. Mohammadi-Samani, A. Behzad-Behbahani, F. Farjadian, Smart pH responsive drug delivery system based on poly (HEMA-co-DMAEMA) nanohydrogel. *Int. J. Pharm.* **552**, 301–311 (2018).
45. P. Tyagi, A. Kumar, Y. Kumar, S. S. Lahiri, Synthesis and characterization of poly (HEMA-MAA) hydrogel carrier for oral delivery of insulin. *J. Appl. Polym. Sci.* **122**, 2004–2012 (2011).
46. E. Luis, H. M. Pan, A. K. Bastola, R. Bajpai, S. L. Sing, J. Song, W. Y. Yeong, 3D printed silicone meniscus implants: Influence of the 3D printing process on properties of silicone implants. *Polymers* **12**, 2136 (2020).
47. C. Zhang, M. Maric, Synthesis of stimuli-responsive, water-soluble poly [2-(dimethylamino) ethyl methacrylate/styrene] statistical copolymers by nitroxide mediated polymerization. *Polymers* **3**, 1398–1422 (2011).
48. H. Zhang, W. Davison, Diffusional characteristics of hydrogels used in DGT and DET techniques. *Anal. Chim. Acta* **398**, 329–340 (1999).
49. E. Reyssat, L. Mahadevan, How wet paper curls. *EPL* **93**, 54001 (2011).
50. D. P. Holmes, M. Roché, T. Sinha, H. A. Stone, Bending and twisting of soft materials by non-homogenous swelling. *Soft Matter* **7**, 5188–5193 (2011).
51. D. J. Beebe, J. S. Moore, J. M. Bauer, Q. Yu, R. H. Liu, C. Devadoss, B.-H. Jo, Functional hydrogel structures for autonomous flow control inside microfluidic channels. *Nature* **404**, 588–590 (2000).

#### Acknowledgments

**Funding:** This work was financially supported by the Ministry of Education, Singapore, under grants R-279-000-576-114 and R-279-000-535-114. F.Y.L. is grateful to the Agency for Science, Technology and Research (A\*STAR) for providing financial support under the PHAROS Advanced Surfaces Programme (grant number 1523700101, IHPC project ID 13001345).

**Author contributions:** S.G., W.C.L., and C.K.A. performed the experiments, characterization, and analyses. F.Y.L. formulated the model and theory of the process. S.S. conceived the project, designed the experiments, and supervised the work. All authors contributed to writing the manuscript. **Competing interests:** The authors declare that they have no competing interests. **Data and materials availability:** All data needed to evaluate the conclusions in the paper are present in the paper and/or the Supplementary Materials. Additional data related to this paper may be requested from the authors.

Submitted 31 August 2020

Accepted 11 February 2021

Published 31 March 2021

10.1126/sciadv.abe5698

**Citation:** S. Gonuguntla, W. C. Lim, F. Y. Leong, C. K. Ao, C. Liu, S. Soh, Performing calculus: Asymmetric adaptive stimuli-responsive material for derivative control. *Sci. Adv.* **7**, eabe5698 (2021).

## Performing calculus: Asymmetric adaptive stimuli-responsive material for derivative control

Spandhana Gonuguntla, Wei Chun Lim, Fong Yew Leong, Chi Kit Ao, Changhui Liu, and Siowling Soh

*Sci. Adv.* **7** (14), eabe5698. DOI: 10.1126/sciadv.abe5698

### View the article online

<https://www.science.org/doi/10.1126/sciadv.abe5698>

### Permissions

<https://www.science.org/help/reprints-and-permissions>

Use of this article is subject to the [Terms of service](#)

---

*Science Advances* (ISSN 2375-2548) is published by the American Association for the Advancement of Science. 1200 New York Avenue NW, Washington, DC 20005. The title *Science Advances* is a registered trademark of AAAS.

Copyright © 2021 The Authors, some rights reserved; exclusive licensee American Association for the Advancement of Science. No claim to original U.S. Government Works. Distributed under a Creative Commons Attribution NonCommercial License 4.0 (CC BY-NC).